Chemical Probing of tDNA^{Phe} with Transition Metal Complexes: A Structural Comparison of RNA and DNA†

Ai Ching Lim and Jacqueline K. Barton*

Division of Chemistry and Chemical Engineering, California Institute of Technology, Pasadena, California 91125

Received June 1, 1993; Revised Manuscript Received August 9, 1993®

ABSTRACT: The three-dimensional folding of tDNA^{Phe} has been examined and compared to native tRNA^{Phe} using a series of shape-selective transition metal complexes as chemical probes of nucleic acid structure. $Rh(phen)_2phi^{3+}$ (phen = phenanthroline, phi = 9,10-phenanthrenequinonediimine), which targets sites of tertiary interaction in tRNA^{Phe}, cleaves specifically at similar sites on tDNA^{Phe}. However, this rhodium complex also targets 5′-pyr-pyr-pur-3′ sites within the acceptor and anticodon stems of tDNA; $Rh(phen)_2phi^{3+}$ generally targets 5′-pyr-pyr-pur-3′ sites in B-form duplex DNA. On tRNA^{Phe}, $Rh(DIP)_3^{3+}$ (DIP = 4,7-diphenyl-1,10-phenanthroline) specifically cleaves C70, which neighbors a GU mismatch, and targets Ψ55 as well, within the hydrophobic region of tRNA^{Phe}. On tDNA^{Phe} no specific cleavage by $Rh(DIP)_3^{3+}$ is observed. The cleavage studies, taken together, indicate that globally the tertiary folding of tDNA^{Phe} resembles that of tRNA^{Phe}. However, the double helical regions of the DNA analog differ from tRNA^{Phe}, likely in adopting a more B-like conformation. As a consequence, the GT mismatch within the acceptor stem of tDNA does not present the same recognition elements as in tRNA, and the GT mismatch is no longer recognized by the shape-selective rhodium complex. The present work underscores the utility of applying DNA analogs to studies of RNA structure and function, since the general folding characteristics of the two polymers are likely to be similar. However, structural probing with transition metal complexes offers a valuable companion to such experiments, since the shape-selective probes, with sensitivity, may be used to delineate locally on the polymer those regions which may differ in structure.

Substantial interest is focused on understanding the three-dimensional folding of RNAs. This understanding is essential in delineating RNA recognition and reactivity. Despite recent advances in synthetic methodology (Usman et al., 1987, 1988; Scaringe et al., 1990; Gasparutto et al., 1992; Milligan et al., 1987), RNA synthesis, either chemical or enzymatic, is not easily accomplished in pure form. In addition, RNA is prone to degradation by nucleases, and few structural probes are available to characterize the products once obtained. In contrast, stable DNA polymers may be prepared in high yield, and both enzymatic and chemical probes are available for their characterization. Given these considerations, many laboratories have begun studies of DNA analogs of RNA polymers (Khan & Roe, 1988; Perreault et al., 1989) or of deoxyribonucleotide polymers containing ribonucleotides at selected positions (Perreault & Altman, 1992; Yang et al., 1992).

But how similar is DNA to RNA, structurally and functionally? Studies on the hammerhead ribozyme have shown that the deoxy analog of a substrate oligonucleotide bearing only a ribonucleotide at the cleavage site is active (Dahm & Uhlenbeck, 1990). The all-deoxy hammerhead domain is inactive, but an oligodeoxynucleotide containing as few as four ribonucleotides in the catalytic domain shows activity (Yang et al., 1992). In addition, an all-DNA external guide sequence can make a potential substrate susceptible to cleavage by RNase P (Perreault & Altman, 1992). Thus, where the 2′-OH is not directly involved in the chemistry of the cleavage site, the secondary and tertiary structure must be conserved to some degree. It has also been demonstrated that tDNAs[1] may be aminoacylated by their cognate aminoacyl synthetases with the correct amino acids in the three cases (phenylalanine, lysine, and methionine) tried thus far, as long as the 3′-riboadenosine is retained (Khan & Roe, 1988; Perreault et al., 1989). Thus the ribose backbone is not required for aminoacylation. Kinetic analysis of aminoacylation of mutant yeast tRNA^{Phe} transcripts (Sampson et al., 1992) has shown that the G20, G34, A35, A36, and G73 nucleotides are the major recognition sites; these five nucleotides must, therefore, still be positioned essentially correctly for aminoacylation in the deoxynucleotide analog. It has also been established through studies utilizing mung bean nuclease and the restriction endonucleases *Hha*I and *Cfo*I (Paquette et al., 1990) that the classic cloverleaf structure is retained in these tRNA analogs.

In view of the wealth of knowledge about tRNA^{Phe} structure (Kim et al., 1974; Quigley & Rich, 1976) and its interactions with its cognate synthetase, we decided to examine in greater structural detail the parallels between tRNA^{Phe} and a chemically synthesized tDNA^{Phe} using a series of chemical probes for local nucleic acid structure. In our laboratory, transition metal complexes have been designed based upon *shape selection* as *local* structural probes for both DNA and RNA (Pyle & Barton, 1990; Chow & Barton, 1992a). Furthermore, the coupling of photoactivated strand cleavage to this recognition provides a sensitive means to mark structurally distinct regions with single-nucleotide resolution. Figure 1 illustrates the shape-selective probes bis(phenanthroline)(9,10-phenanthrenequinonediimine)rhodium(III) [$Rh(phen)_2phi^{3+}$], tris(4,7-diphenyl-1,10-phenanthroline)rhodium-

† We are grateful to the National Institutes of Health (GM33309) for financial support of this work.

* Author to whom correspondence should be addressed.

® Abstract published in *Advance ACS Abstracts,* October 1, 1993.

[1] tDNAs are synthetic DNA oligomers, analogs of particular full-length tRNAs, with dT substituted in the positions occupied by ribouridine or its derivatives. In addition, unmodified bases are used instead of modified ones in the case of the tDNA studied in our laboratory.

0006-2960/93/0432-11029$04.00/0

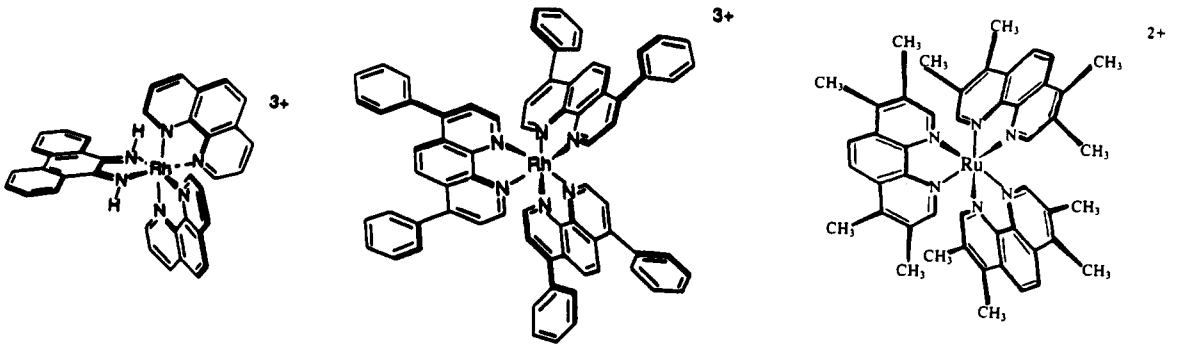

FIGURE 1: Schematic illustration of the shape-selective probes $Rh(phen)_2phi^{3+}$, $Rh(DIP)_3^{3+}$, and $Ru(TMP)_3^{2+}$.

(III) [$Rh(DIP)_3^{3+}$], and tris(3,4,7,8-tetramethylphenanthroline)ruthenium(II) [$Ru(TMP)_3^{2+}$]. $Rh(phen)_2phi^{3+}$ has been shown to intercalate in the major groove of double-helical DNA at 5′-pyr-pyr-pur-3′ steps (Pyle et al., 1989, 1990; Sitlani et al., 1992; David & Barton, 1993) and, consistent with this recognition, to target sites of tertiary interaction in folded RNAs (Chow & Barton, 1990; Chow et al., 1992a,b). $Rh(DIP)_3^{3+}$ targets unusual DNA tertiary structures, such as cruciforms, Z-DNA, and Holliday junctions (Kirshenbaum et al., 1988; Lee & Barton, 1993), while it targets primarily GU mismatches in RNAs (Chow & Barton, 1992b). $Ru(TMP)_3^{2+}$ binds against the shallow minor groove of RNA and DNA double helices which are A-like in character (Mei & Barton, 1986, 1988; Chow & Barton, 1990).

Here we report the application of these different shape-selective probes to compare and contrast the structure of $tDNA^{Phe}$ and $tRNA^{Phe}$. In general we find the overall folding of the tDNA to resemble that of tRNA, but local variations and potential recognition elements differ. In particular, double-helical regions of the molecule differ in that these regions adopt primarily the B-conformation.

MATERIALS AND METHODS

$tRNA^{Phe}$. Native yeast $tRNA^{Phe}$ from brewer's yeast (Boehringer Mannheim) was 3′-end-labeled with cytidine 3′,5′-[5′-^{32}P]bisphosphate using T4 RNA ligase (England & Uhlenbeck, 1978). It was then gel purified on a 10% denaturing polyacrylamide gel, located by autoradiography, excised, and eluted from the gel slice in 45 mM Tris, 45 mM boric acid, and 1.25 mM EDTA, pH 8.0. The eluted $tRNA^{Phe}$ was ethanol precipitated twice and stored frozen in 10 mM Tris-HCl, pH 7.5.

$tDNA^{Phe}$. $tDNA^{Phe}$ was chemically synthesized on a 1-μM scale on an Applied Biosystems 392 DNA/RNA synthesizer using the phosphoramidite method. Unusual bases were not incorporated into the polymer. The oligonucleotide was then purified twice by HPLC, first with the dimethoxytrityl (DMT) group on and subsequently with the DMT group off, using a C_{18} column (Dynamax). The oligonucleotide was then purified on a 10% denaturing polyacrylamide gel, located by UV shadowing, excised, and eluted from the gel in 45 mM Tris, 45 mM boric acid, and 1.25 mM EDTA, pH 8.0. The eluted tDNA was concentrated by a Centricon 10 (Amicon) device, desalted by washing twice with water, and stored in 10 mM Tris-HCl, pH 7.5. The purified oligonucleotide has a UV maximum at 257 nm and an extinction coefficient at 260 nm of 8500 M^{-1} cm^{-1}/nucleotide. The tDNA was then 3′-end-labeled with [α-^{32}P]ddATP using terminal deoxytransferase or 5′-end-labeled with [γ-^{32}P]ATP using T4 polynucleotide kinase. The labeled material was gel purified by the same method as for $tRNA^{Phe}$ and stored frozen in 10 mM Tris-HCl, pH 7.5.

Cleavage Reactions. $[Rh(phen)_2phi]Cl_3$, $[Rh(DIP)_3]Cl_3$, $[Ru(TMP)_3]Cl_2$, and $[Ru(phen)_3]Cl_2$ were prepared in our laboratory by published procedures (Chow & Barton, 1992a). All metal stock solutions were freshly prepared in either ethanol or 10 mM Tris-HCl, pH 7.5. The end-labeled $tRNA^{Phe}$ and $tDNA^{Phe}$ were renatured by heating to 70 °C for 1 min in 10 mM Tris-HCl, pH 7.5 (10 mM $MgCl_2$ optional), and slowly cooling to room temperature prior to use. A typical 20-μL cleavage mixture contained labeled RNA or DNA, 2.5–10 μM metal complex (freshly diluted in H_2O), and the appropriate buffer (50 mM Tris, 20 mM NaOAc, and 18 mM NaCl, pH 7.0, or 5 mM Tris and 50 mM NaCl, pH 7.0; 10 mM $MgCl_2$ optional to both buffers) and was brought to a final concentration of 100 μM in nucleotides with either carrier $tRNA^{Phe}$ or $tDNA^{Phe}$. The mixture was incubated for a maximum of 5 min at room temperature and was then irradiated at 365 nm in the case of the $Rh(phen)_2phi^{3+}$ mixtures and 313 nm for the $Rh(DIP)_3^{3+}$ mixtures at ambient temperature using a 1000-W Hg/Xe lamp and monochromator (Oriel Model 77250). The $Ru(TMP)_3^{2+}$ and $Ru(phen)_3^{2+}$ mixtures were irradiated at 442 nm using a He–Cd laser (Liconix Model 4200 NB) at 19 mW for 10–30 min at ambient temperature. The reaction mixtures were ethanol precipitated and washed at least three times with ethanol to remove buffer salts and then dried on a SpeedVac Concentrator (Savant). In addition, the dry ruthenium complex mixtures were treated with either 1 M piperidine in H_2O (for DNA) at 90 °C or 1 M aniline (for RNA) at 60 °C for 30 min to reveal sites of modification.

Sequencing Gels. The cleavage products were analyzed on 20% polyacrylamide–8 M urea gels and viewed by autoradiography. The full-length $tRNA^{Phe}$ and its cleavage products were identified by coelectrophoresing with the products of $Ru(phen)_3^{2+}$ (G-specific) reactions (Chow & Barton, 1990) and diethyl pyrocarbonate (DEPC) (A-specific) and hydrazine (U-specific) reactions (Peattie, 1979), and the full-length $tDNA^{Phe}$ and its cleavage products were identified by coelectrophoresing with the products of piperidine formate (A+ G-specific) and hydrazine hydrate (C+T-specific) Maxam–Gilbert reactions (Sambrook et al., 1989). The fragments produced by the metal complex cleavage possess 3′- and 5′- phosphate termini and thus could be directly compared with the chemical sequencing lanes.

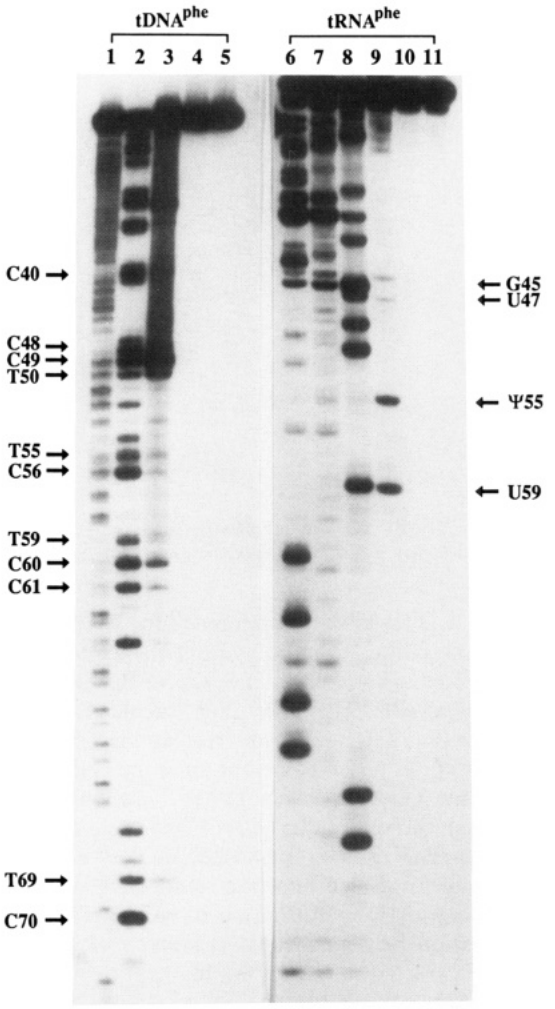

FIGURE 2: Autoradiogram showing cleavage of 3′-^{32}P-labeled tDNA^{Phe} (lanes 1–5) and tRNA^{Phe} (lanes 6–11) by Rh(phen)$_2$phi^{3+} in 50 mM Tris, 20 mM NaOAc, and 18 mM NaCl, pH 7.0. Lanes 1 and 2: A+G and C+T reactions on tDNA^{Phe}, respectively. Lane 3: cleaved tDNA^{Phe} after incubation with 5 μM Rh(phen)$_2$phi^{3+} and irradiation for 4 min at 365 nm. Lane 4: labeled DNA with 5 μM Rh(phen)$_2$phi^{3+} but without irradiation. Lane 5: labeled DNA irradiated for 4 min at 365 nm in the absence of metal complex. Lanes 6, 7, and 8: A-, G-, and U-specific reactions on labeled tRNA^{Phe}, respectively. Lane 9: cleaved tRNA^{Phe} after incubation with 5 μM Rh(phen)$_2$phi^{3+} and irradiation for 10 min at 365 nm. Lane 10: labeled RNA with 5 μM Rh(phen)$_2$phi^{3+} but without irradiation. Lane 11: labeled RNA after irradiation for 10 min at 365 nm in the absence of metal complex.

RESULTS

Cleavage of tDNA^{Phe} by Rh(phen)$_2$phi^{3+}. Cleavage sites induced by Rh(phen)$_2$phi^{3+} on the folded tDNA were determined using gel electrophoresis after reaction with tDNA either labeled at the 3′- or 5′-terminus. Specific sites of cleavage are observed on tDNA^{Phe} which are similar but not identical to those found upon irradiation of tRNA^{Phe} with Rh(phen)$_2$phi^{3+} (Chow et al., 1992a). Figure 2 shows cleavage of 3′-labeled tDNA^{Phe} and tRNA^{Phe}. At a Rh(phen)$_2$phi^{3+} concentration of 5 μM after 5 min of irradiation, several strong sites are visible on tDNA^{Phe}. Strongest cleavage occurs at residues C28, C48, and C49. Rhodium-induced cleavage is also seen at A29, C40, T50, and C60, and weak cleavage sites may also be discerned at C32, G45, G46, T55, C56, T59, C61, T69, and C70. Identical sites of cleavage are apparent in experiments conducted with 5′-labeled tDNA, where, in addition, another site is seen at residue A9. When cleavage experiments were conducted on denatured tDNA (heated to 90 °C for 5 min prior to irradiation and irradiated at that temperature), no cleavage was seen. This observation is consistent with the requirement of the folded structure for recognition and cleavage by the metal complex. It should be noted that no difference in cleavage patterns was observed on tDNA upon the addition of 10 mM $MgCl_2$ to the buffer; in contrast, some loss of cleavage was observed at tertiary sites on tRNA^{Phe} (Chow et al., 1992a). It is also noteworthy that shorter irradiation times are generally required for the cleavage of tDNA^{Phe} compared to tRNA^{Phe}, implying that the DNA is cleaved more efficiently than the RNA.

Table I: Comparison of Rh(phen)$_2$phi^{3+} Cleavage Sites on tRNA^{Phe}, the tRNA^{Phe} transcript, and tDNA^{Phe}

species	cleavage sites[a]	location
tRNA^{Phe}	**G22**, **G45**, *m^{7}G46*, **U47**, *C48*	triply bonded core
	Ψ55, **U59**	T loop
tRNA^{Phe} transcript	*C27*, *A36*, *G37*, A38	anticodon stem/loop
	G22, *G45*, *G46*, **U47**, **C48**	triply bonded core
	U55, **U59**	T loop
tDNA^{Phe}	A9	D loop
	C28, A29, *C32*, C40	anticodon stem/loop
	G45, *G46*, **C48**, **C49**, T50	triply bonded core
	T55, *T56*, *T59*, C60, *C61*	T loop
	T69, *C70*	acceptor stem

[a] Strong cleavage sites are in boldface; very weak sites are italicized.

As illustrated in Table I and Figure 3, the specific sites obtained on tDNA^{Phe} may be contrasted to those sites targeted by the rhodium complex on the native tRNA, also shown in the gel, as well as to those sites found on the tRNA^{Phe} transcript, which, like the tDNA analog, lacks modified bases (Chow et al., 1992a). It is apparent that the same regions of the molecule are targeted on the tRNA and tDNA analogs. However, the relative intensities of cleavage among the regions differ for the tRNAs versus tDNA, and some regions on tDNA are targeted which are not evident on the tRNAs. For example, on tRNA^{Phe} cleavage is evident primarily within two regions of the molecule, most strongly within the folded corner of the molecule where the D and TΨC loops interact at Ψ55 and U59 and also, but more weakly, along the central region created through the extensive tertiary interactions centered around m^{7}G46. On tDNA, instead, it is this central tertiary structure which is most strongly targeted, and the primary site of cleavage is shifted to C48. Cleavage is also evident on tDNA at T55 and T59 but is again shifted in that greater cleavage is evident at C56 and C60. The tRNA transcript represents an intermediate case; here cleavage is also found in both tertiary folds of the molecule, despite the replacement of Ψ55 by U55, and within the central portion of the molecule, where cleavage is centered on U47.

The sites not present on the tRNAs but which are targeted by the rhodium complex on tDNA^{Phe} occur along the stem regions. On the tDNA^{Phe} acceptor and anticodon stems, there is a strong correspondence between 5′-pyr-pyr-pur-3′ steps and cleavage sites, as shown in Table II. On B-form DNA these sites are characteristically recognized by Rh(phen)$_2$phi^{3+} (Sitlani et al., 1992). For example, Rh(phen)$_2$phi^{3+} targets 5′-CCA-3′ on the anticodon stem, a sequence which is not cleaved on tRNA^{Phe} but which represents the primary recognition site for the complex on duplex DNA (Sitlani et al., 1992). This targeting is therefore consistent with the notion that the tDNA differs in structure from the tRNA in adopting a more B-like conformation within the double helical acceptor and anticodon stems. This observation is also consistent with an NMR study which indicated that an RNA pentameric helix with the sequence (5′-rCUGUG/5′-rCACAG), corresponding to the TΨC stem in yeast tRNA^{Phe}, adopts an A-form

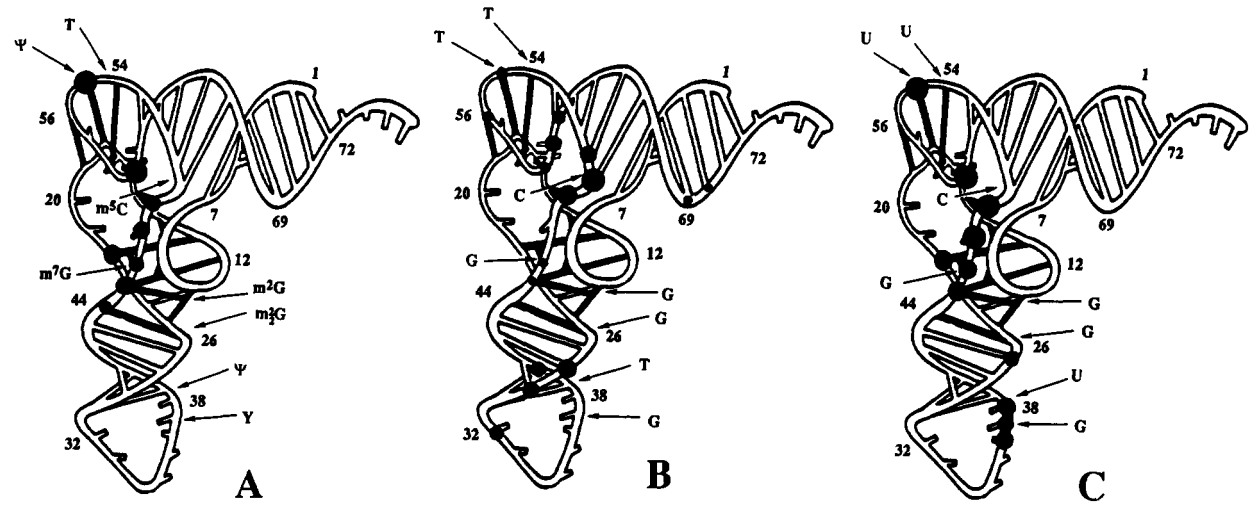

FIGURE 3: Ribbon diagrams showing $Rh(phen)_2phi^{3+}$ cleavage sites on $tRNA^{Phe}$ (A), $tDNA^{Phe}$ (B), and $tRNA^{Phe}$ transcript (C). The solid circles indicate the sites of cleavage, with the circle size reflecting the relative cleavage intensity. Arrows indicate the bases which are modified in the native $tRNA^{Phe}$.

Table II: Correspondence of Selected Cleavage Sites on $tDNA^{Phe}$ to 5′-pyr-pyr-pur-3′ Sites in Double-Helical Regions

cleavage site(s)	5′-pyr-pyr-pur-3′ steps	location
A9	T7-T8-A9	acceptor stem/D loop
C28, A29	C27-C28-A29	anticodon stem
C32	C32-T33-G34	anticodon loop
C40	C40-T41-G42	anticodon stem
T69, C70	T69-C70-G71	acceptor stem

conformation, whereas the analogous DNA pentamer is found to adopt the B-form conformation (Hall & McLaughlin, 1991). It is noteworthy, however, that these sites are generally weaker in intensity than the sites of tertiary interaction. Furthermore, the cleavage is weaker in intensity than is commonly observed in DNA oligonucleotides.

Cleavage of $tDNA^{Phe}$ by $Rh(DIP)_3^{3+}$. $Rh(DIP)_3^{3+}$ has been shown to target selectively two sites on $tRNA^{Phe}$, Ψ55 and C70. Targeting of Ψ55 appears to depend upon the complex tertiary folding of the tRNA where the D and TΨC loops interact; in the tRNA transcript, which lacks the pseudouracil, $Rh(DIP)_3^{3+}$ targets U55 (Chow et al., 1992a). Importantly, targeting of C70 appears to depend upon the recognition of the neighboring GU mismatch. In several RNAs, $Rh(DIP)_3^{3+}$ has been shown to target the base to the 3′-side of a GU mismatch within double-helical regions (Chow & Barton, 1992b). In the absence of a strong recognition site, on DNAs a faint reaction at guanines has generally been found (Lee & Barton, 1993).

The comparison in cleavage by $Rh(DIP)_3^{3+}$ on $tRNA^{Phe}$ and $tDNA^{Phe}$ is quite striking, as shown in Figure 4. Although strong cleavage is evident by the rhodium complex at Ψ55 and C70 on $tRNA^{Phe}$, only a faint reaction at guanines is evident on $tDNA^{Phe}$. The same absence of specific cleavage on $tDNA^{Phe}$ is evident with higher concentrations of rhodium and longer irradiation times or with the addition of 10 mM $MgCl_2$.

Cleavage of $tDNA^{Phe}$ by $Ru(TMP)_3^{2+}$ and by $Ru(phen)_3^{2+}$. $Ru(TMP)_3^{2+}$ has been shown to selectively bind A-form helical regions of RNAs and DNAs (Mei & Barton, 1986, 1988). Since $Ru(TMP)_3^{2+}$ promotes nucleic acid strand cleavage in a nucleic acid base-dependent reaction mediated by singlet oxygen, comparative cleavage experiments are always carried out using $Ru(phen)_3^{2+}$, which also promotes nucleic acid cleavage with irradiation in a reaction mediated by singlet oxygen but which shows no preference for A-form regions because of its smaller size and hydrophobicity compared to $Ru(TMP)_3^{2+}$. Earlier studies have shown that some differences in cleavage are evident between $Ru(phen)_3^{2+}$ and $Ru(TMP)_3^{2+}$ on $tRNA^{Phe}$, in that some protection from cleavage by $Ru(TMP)_3^{2+}$ is observed neighboring the helical regions of the molecule (Chow & Barton, 1990). No strong selectivity was apparent, however. On $tDNA^{Phe}$, no differences in cleavage between $Ru(phen)_3^{2+}$ and $Ru(TMP)_3^{2+}$ are observed (data not shown). Since some differences are evident with tRNA but not with tDNA, this result also supports a difference in conformation between helical regions of $tRNA^{Phe}$ and $tDNA^{phe}$.

DISCUSSION

Comparisons in Structures of $tRNA^{Phe}$ and $tDNA^{Phe}$. Chemical probing of the structure of $tDNA^{Phe}$ with the shape-selective transition metal complexes indicates that the tertiary folding of the DNA analog globally resembles that of $tRNA^{Phe}$ but that some differences in local conformation are evident. The metal complexes provide site-selective probes of different regions of the molecule: the acceptor and anticodon stems, the central region where triply bonded bases interact, and the region where the D and TΨC loops associate. A computer-graphic representation of the crystal structure of $tRNA^{Phe}$ which highlights the similarities and differences between $tDNA^{Phe}$ and $tRNA^{Phe}$ as probed by the various rhodium complexes is shown in Figure 5.

Both $Rh(phen)_2phi^{3+}$ and $Rh(DIP)_3^{3+}$ provide probes of the tertiary folding in the D and TΨC loops. In $tRNA^{Phe}$, intense cleavage by $Rh(phen)_2phi^{3+}$ is observed at Ψ55 and U59. On tDNA, cleavage is maintained by $Rh(phen)_2phi^{3+}$ in the vicinity of T55 and T59 but is shifted by one base to T56 and C60 and is of lower intensity. With $Rh(DIP)_3^{3+}$, despite strong cleavage at Ψ55 in $tRNA^{Phe}$ and consistent cleavage in a series of tRNA mutants containing substitutions within that region of the molecule, no specific cleavage in the vicinity of T55 is detectable on tDNA. These results may indicate that the basic folding within this region is maintained on the DNA analog but perhaps is less flexible in structure and therefore less accessible to association with the bulky $Rh(DIP)_3^{3+}$. This point is consistent also with the differences seen in reactivity of tDNA versus tRNA in the presence and absence of magnesium ion. Cleavage in this region is not

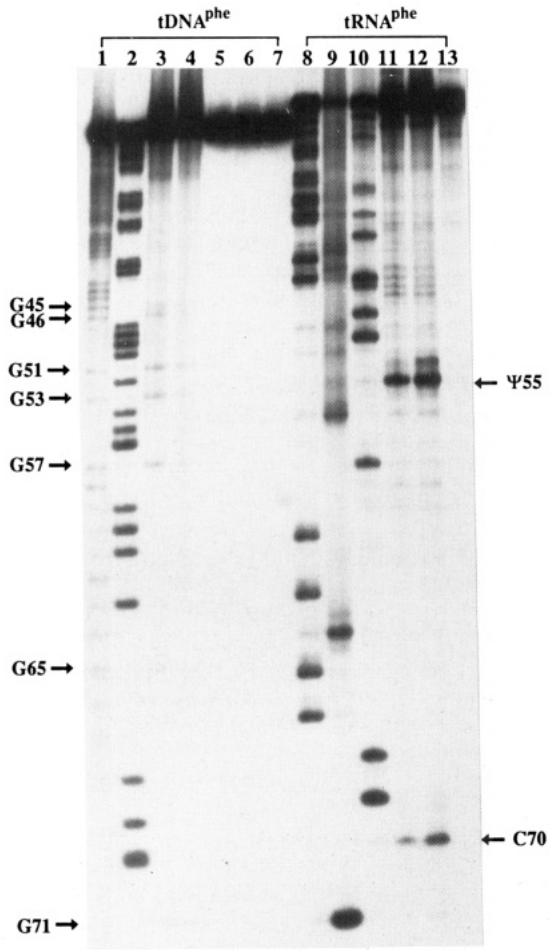

FIGURE 4: Autoradiogram showing cleavage of 3′-^{32}P-labeled $tDNA^{Phe}$ and $tRNA^{Phe}$ by $Rh(DIP)_3^{3+}$ in 50 mM Tris, 20 mM NaOAc, and 18 mM NaCl, pH 7.0. Lanes 1 and 2: A+G and C+T reactions, respectively, on $tDNA^{Phe}$. Lane 3: cleaved $tDNA^{Phe}$ after incubation with 2.5 μM $Rh(DIP)_3^{3+}$ and irradiation for 6 min at 313 nm. Lane 4: cleaved $tDNA^{Phe}$ after incubation with 10 μM $Rh(DIP)_3^{3+}$ and irradiation for 10 min at 365 nm. Lane 5: labeled DNA with 10 μM $Rh(DIP)_3^{3+}$but without irradiation. Lane 6: labeled DNA upon irradiation for 6 min at 313 nm. Lane 7: labeled DNA without metal or irradiation. Lanes 8, 9, and 10: A-, G-, and U-specific reactions, respectively, on $tRNA^{Phe}$. Lane 11: cleaved $tRNA^{Phe}$ after incubation with 2.5 μM $Rh(DIP)_3^{3+}$ and irradiation for 6 min at 313 nm. Lane 12: cleaved $tRNA^{Phe}$ after incubation with 10 μM $Rh(DIP)_3^{3+}$ and irradiation for 10 min at 365 nm. Lane 13: cleaved $tRNA^{Phe}$ after incubation with 10 μM $Rh(DIP)_3^{3+}$but without irradiation.

affected by Mg^{2+} on $tDNA^{Phe}$ but is inhibited to some extent on $tRNA^{Phe}$ (Chow et al., 1992a).

The overall structure and folding of tRNA is also defined by the triple base interactions in the central core of the molecule, and on $tRNA^{Phe}$ these sites are specifically targeted by $Rh(phen)_2phi^{3+}$. On tDNA this region is also specifically targeted, and indeed with the DNA analog this region represents the primary area for rhodium-induced cleavage. That this region in $tDNA^{Phe}$ is specifically recognized by $Rh(phen)_2phi^{3+}$ supports the notion that the DNA analog adopts an overall folded structure like that of tRNA. Nonetheless, the details of this folding differ. Cleavage on tDNA occurs strongly at positions C48 and C49, compared to the tRNA transcript where cleavage is centered on U47 and the native $tRNA^{Phe}$ where cleavage is found most strongly around m^7G46.

The clear difference in targeting of the DNA and RNA analogs is apparent within the double-helical stem regions. $Rh(phen)_2phi^{3+}$ targets 5′-pyr-pyr-pur-3′ sites on B-form DNA since these sites are open and accessible in the major groove

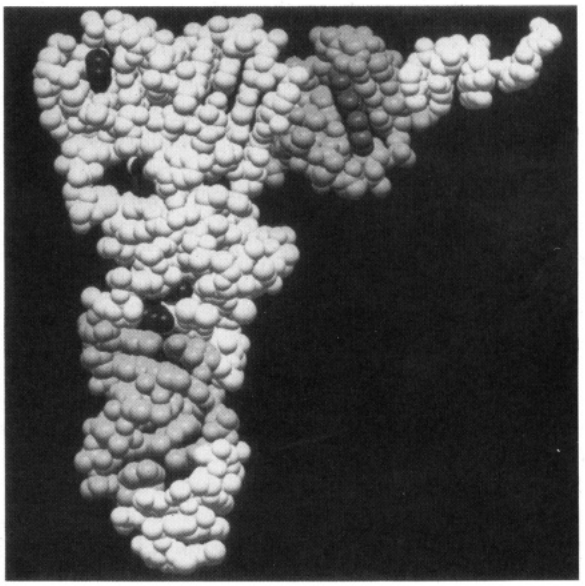

FIGURE 5: Computer-graphic representation of the crystal structure of $tRNA^{Phe}$ highlighting the similarities and differences between $tDNA^{Phe}$ and $tRNA^{Phe}$ as probed by rhodium complexes. Double-helical regions which are A-form in $tRNA^{Phe}$ and B-form in $tDNA^{Phe}$ are shown in light gray. The GU mismatch recognized by $Rh(DIP)_3^{3+}$ on $tRNA^{Phe}$ is shown in darker gray; the corresponding GT mismatch on DNA is not recognized. Bases involved in tertiary and/or triple interactions which are recognized by $Rh(phen)_2phi^{3+}$ on $tRNA^{Phe}$, $tRNA^{Phe}$ transcript, and $tDNA^{Phe}$ are shown in black.

for intercalative binding (David & Barton, 1993; Sitlani et al., 1992). On $tRNA^{Phe}$ and a series of tRNA mutant transcripts, no specific cleavage within the acceptor or anticodon stems by $Rh(phen)_2phi^{3+}$ is observed (Chow et al., 1992a). In sharp contrast, on tDNA specific cleavage is observed at 5′-pyr-pyr-pur-3′ sites within the putatively double-helical regions. This targeting therefore indicates that, like the tRNA analogs, tDNA contains double-helical regions, but unlike the tRNA analogs, tDNA contains B-form helical regions. For tDNA the major groove is accessible to intercalation, whereas in tRNAs in these double-helical regions the major groove is not accessible, likely because the helix is more A-like in character. Experiments with $Ru(TMP)_3^{2+}$ also support this conclusion.

It is noteworthy that the anticodon loop in tDNA resembles that of neither the native $tRNA^{Phe}$ nor the $tRNA^{Phe}$ transcript, on the basis of cleavage by $Rh(phen)_2phi^{3+}$. As may be evident in Figure 3, on tDNA, cleavage occurs within 5′-C32-T33-G34-3′, a 5′-pyr-pyr-pur-3′ step, suggesting that this loop in tDNA may maintain the B-like helicity of the anticodon stem. No specific cleavage is apparent in the anticodon loop of the native tRNA, and some cleavage, though different, is evident in the more flexible loop of the tRNA transcript.

Also of particular note is the absence of recognition of the GT mismatch within the anticodon stem of tDNA by $Rh(DIP)_3^{3+}$. On $tRNA^{Phe}$ and microhelices derived from it, $Rh(DIP)_3^{2+}$ has been shown to target GU mismatches, specifically cleaving to the 3′-side of the U, within double-helical regions (Chow & Barton, 1992b). A GU mismatch does not stack well with the flanking base pair to the 3′-side of the U, and the wobble-paired U residue is pushed away from the helix interior into the major groove of RNA. Yet no specific recognition of the GT mismatch in tDNA by $Rh(DIP)_3^{3+}$ is evident. The absence of recognition may be a consequence of the change in conformation of the region to the B-form, where perhaps the GT wobble does not present the structural perturbation (Quignard et al., 1989) that is apparent within

the A-form helix. We cannot, however, eliminate the effects on recognition presented by the methyl group on T. This difference in recognition between RNA and DNA is important, since it is known that the G3–U70 mismatch is critical for identity of *Escherichia coli* $tRNA^{Ala}$ (Hou & Shimmel, 1988, 1989) and $tRNA^{Asp}$ (Ruff et al., 1991). The fact that the $tDNA^{Phe}$ is still recognized by its cognate synthetase (Khan & Roe, 1988) implies that the GU mismatch is not crucial for the identity of yeast $tRNA^{Phe}$. It would be interesting to compare aminoacylation experiments on *E. coli* $tDNA^{Ala}$ and $tRNA^{Ala}$. GU mismatches appear generally to serve as recognition elements in the interactions of proteins and RNA. The substitution of deoxy analogs within RNA molecules must therefore take this effect on the structure of the GU mismatch into account. It is not unreasonable to consider that, like $Rh(DIP)_3^{3+}$, RNA-binding proteins may also lose an ability to distinguish the GU mismatch within a DNA polymer.

Implications for Studies of RNA and DNA Structure. Because of their relative ease of synthesis and greater stability, DNA analogs have increasingly been exploited in studies to explore RNA structure, reaction, and function (Dahm & Uhlenbeck, 1990; Yang et al., 1992; Perreault & Altman, 1992). Yet few structural probes are available to examine, locally along the polymer, the structural consequences in converting from the ribose to the deoxyribose form. The present study illustrates the utility of transition metal complexes in comparing with high sensitivity the differences and similarities in the local structure of DNA and RNA analogs. The results indicate that globally the structures of tRNA and tDNA analogs resemble one another. Yet distinctions are apparent, in particular within double helical regions. Moreover, detailed structural perturbations, such as the GU mismatch, may vary considerably and thus offer different distinguishing elements for protein recognition. The results described here therefore provide support for the application of DNA analogs in studies of RNA structure and function. However, the present work also serves to underscore the importance and powerful application of transition metal complexes to probe local variations in RNA and DNA structure and how, if chemical probing is conducted in concert with studies of RNA function, the results of such studies may be far more clearly understood.

REFERENCES

Chow, C. S., & Barton, J. K. (1990) *J. Am. Chem. Soc. 112*, 2839–2841.

Chow, C. S., & Barton, J. K. (1992a) *Methods Enzymol. 212*, 219–241.

Chow, C. S., & Barton, J. K. (1992b) *Biochemistry 31*, 5424–5429.

Chow, C. S., Behlen, L. S., Uhlenbeck, O. C., & Barton, J. K. (1992a) *Biochemistry 31*, 972–982.

Chow, C. S., Hartmann, K. M., Rawlings, S. L., Huber, P. W., & Barton, J. K. (1992b) *Biochemistry 31*, 3534–3542.

Dahm, S. C., & Uhlenbeck, O. C. (1990) *Biochimie 72*, 819–823.

David, S. D., & Barton, J. K. (1993) *J. Am. Chem. Soc. 115*, 2984–2985.

England, T. E., & Uhlenbeck, O. C. (1978) *Nature 275*, 560–561.

Gasparutto, D., Livache, T., Duplaa, A.-M., Bazin, H., Favario, S., Guy, A., Molko, D., Roget, A., & Teoule, R. (1992) *C. R. Acad. Sci. 315*, 1–6.

Hall, K. B., & McLaughlin, L. W. (1991) *Biochemistry 30*, 10606–10613.

Hou, Y.-M., & Schimmel, P. (1988) *Nature 333*, 140–145.

Hou, Y.-M., & Schimmel, P. (1989) *Biochemistry 28*, 6800–6804.

Khan, A. S., & Roe, B. A. (1988) *Science 241*, 76–79.

Kim, S.-H., Sussman, J. L., Suddath, F. L., Quigley, G. J., McPherson, A., Wang, A. H. J., Seeman, N. C., & Rich, A. (1974) *Proc. Natl. Acad. Sci. U.S.A. 71*, 4970–4974.

Kirshenbaum, M. R., Tribolet, R., & Barton, J. K. (1988) *Nucleic Acids Res. 16*, 7943–7959.

Lee, I., & Barton, J. K. (1993) *Biochemistry* (in press).

Mei, H.-Y., & Barton, J. K. (1986) *J. Am. Chem. Soc. 108*, 7414–7416.

Mei, H.-Y., & Barton, J. K. (1988) *Proc. Natl. Acad. Sci. U.S.A. 85*, 1339–1343.

Milligan, J. F., Groebe, D. R., Witherell, G. W., & Uhlenbeck, O. C. (1987) *Nucleic Acids Res. 15*, 8783–8798.

Paquette, J., Nicoghosian, K., Qi, G., Beauchemin, N., & Cedergren, R. (1990) *Eur. J. Biochem. 189*, 259–265.

Peattie, D. A. (1979) *Proc. Natl. Acad. Sci. U.S.A. 76*, 1760–1764.

Perreault, J.-P., & Altman, S. (1992) *J. Mol. Biol. 226*, 399–409.

Perreault, J.-P., Pon, R. T., Jiang, M., Usman, N., Pika, J., Ogilvie, K. K., & Cedergren, R. (1989) *Eur. J. Biochem. 186*, 87–93.

Pyle, A. M., & Barton, J. K. (1990) *Prog. Inorg. Chem. 38*, 413–473.

Pyle, A. M., Long, E. C., & Barton, J. K. (1989) *J. Am. Chem. Soc. 111*, 4520–4522.

Pyle, A. M., Morii, T., & Barton, J. K. (1990) *J. Am. Chem. Soc. 112*, 9432–9434.

Quigley, G. J., & Rich, A. (1976) *Science 194*, 796–806.

Quignard, E., Fazakerley, G. V., van der Marel, G., van Boom, J. H., & Guschlbauer, W. (1987) *Nucleic Acids Res. 15*, 3397–3409.

Ruff, M., Krishnaswamy, S., Boeglin, M., Poterszman, A., Mitscher, A., Podjarny, A., Rees, B., Thierry, J. C., & Moras, D. (1991) *Science 252*, 1682–1689.

Sambrook, J., Fritsch, E. F., & Manniatis, T. (1989) *Molecular Cloning: A Laboratory Manual* (2nd ed.) Cold Spring Harbor Laboratory Press, Cold Spring Harbor, NY.

Sampson, J. R., Behlen, L. S., DiRenzo, A. B., & Uhlenbeck, O. C. (1992) *Biochemistry 31*, 4161–4167.

Scaringe, S. A., Francklyn, C., & Usman, N. (1990) *Nucleic Acids Res. 18*, 5433–5441.

Sitlani, A., Long, E. C., Pyle, A. M., & Barton, J. K. (1992) *J. Am. Chem. Soc. 114*, 2303–2312.

Usman, N., Ogilvie, K. K., Jiang, M. Y., & Cedergren, R. L. (1987) *J. Am. Chem. Soc. 109*, 7845–7854.

Usman, N., Nicoghosian, K., Cedergren, R. L., & Ogilvie, K. K. (1988) *Proc. Natl. Acad. Sci.U.S.A. 85*, 5764–5768.

Yang, J. H., Usman, N., Chartrand, P., & Cedergren, R. (1992) *Biochemistry 31*, 5005–5009.